e-Polymers **2007**, no. 074

http://www.e-polymers.org

ISSN 1618-7229

Structure and properties of styrene-butadiene rubber/ pristine clay nanocomposites prepared by latex compounding method

Mahdi Abdollahi, Ali Rahmatpour, Jamal Aalaie, Homayon Hossein Khanli*

Division of Polymer Science and Technology, Research Institute of Petroleum Industry (RIPI), P. O. Box: 18745-4163, Tehran, Iran, Fax: +98 21 88937006, E-mail: abdollahim@ripi.ir, m_abdollahi@modares.ac.ir

(Received : 16 May, 2007; published: 27 July, 2007)

Abstract: Styrene- butadiene rubber (SBR)/ clay nanocomposites were prepared by mixing the SBR latex with aqueous clay dispersion and co-coagulating the mixture. Tapping mode AFM and XRD were applied to characterize the structure of nanocomposites. It was found that fully exfoliated structure could be obtained by this method only when the low loading of layered silicate (< 10 phr) is used. With increasing the clay content, both non-exfoliated (stacked layers) and exfoliated structures can be observed simultaneously in the nanocomposites. The results of mechanical tests on the vulcanized pure SBR and SBR/ clay nanocomposites showed that the nanocomposites presents better mechanical properties than clay-free SBR vulcanizate. Furthermore, initial modulus, tensile strength, tensile strain at break, hardness (shore A) and tear strength increased with increasing the clay content, indicating the nanoreinforcement effect of clay on the mechanical properties of SBR/ clay nanocomposites. Compared to the clay free SBR vulcanizate, the nanocomposite vulcanizates exhibit a lower tanδ peak value, higher storage modulus and higher tanδ value at the rubbery region (0-60 ^{0}C) which indicate that the elastic responses of pure SBR towards deformation are strongly influenced by the presence of nanodisperced natural sodium montmorillonite layers especially completely exfoliated silicate layers.

Introduction

For many years, high performance elastomers have been prepared by using carbon black, which improves the mechanical property effectively, but unfortunately pollutes the environment and is derived from petroleum. Introduction of a small amount of nanoclay into a polymer matrix improves a variety of properties such as mechanical and barrier properties. Recently, polymer/ clay (layered silicate) nanocomposites have attracted much attention for both academic researchers and industrial applications because they mostly present unexpected properties synergistically obtained from the two components [1-2]. The essence of this development is the nanoscale dispersion [3-4] and the very high aspect ratio of the clay layers [5]. Nowadays rubber/ clay nanocomposites are of great interest because of their excellent gas barrier properties and, more importantly, their much higher strength in comparison with plastics/ clay nanocomposites [6, 7].

This nanoscale dispersion of clay is highly relevant for rubber compounds since their application requires reinforcement with filler. Carbon black and also inorganic minerals (talc, TiO_2, etc.) are usually used to reinforce vulcanized rubbers and to improve the mechanical properties. Carbon black is an excellent reinforcement due

to its strong interaction with rubbers, but its presence especially at high loading often decreases the processability of rubber compounds and unfortunately pollutes the environment and is derived from petroleum.

Different methods have been used to prepare rubber/ layered silicate nanocomposites such as acrylonitrile- butadiene rubber (NBR) [8], ethylene-propylene- diene monomer (EPDM) [9, 10], natural rubber (NR) [11, 12], butadiene rubber (BR) and SBR [13-17]. Generally, in situ polymerization, solution and melt intercalation are the preparation methods of rubber/ clay nanocomposites, wherein organic modified layered silicate must be used. However, considering that the latexes are aqueous polymer dispersions and water is an excellent exfoliating agent for pristine clays, co-coagulating the mixture of rubber latex and layered silicate aqueous suspension (latex compounding method) is an easy method to prepare layered silicate/ rubber nanocomposites wherein pristine clay, i.e. sodium montmorillonite (Na-MMT), is used instead of organic clay [13-14, 18-19].

In recent years, atomic force microscopy (AFM) has been used for imaging of composite materials [20, 21], a technique that does not require any specific preparation of the samples. More specific, we use tapping mode AFM with phase imaging, which is one of the latest developments in scanning probe microscopy.

SBR is an important rubber and used widely in the rubber industry. Zhang et al. prepared SBR/ pristine clay nanocomposite by compounding the rubber latex and aqueous suspension of pristine clay (sodium clay) followed by co-coagulating the mixture [13, 14]. Structure of the nanocomposites was proposed to be a layer bundle of layered silicates whose thickness was 4-10 nm and its aggregation formed by several or many layer bundles, since X- ray diffraction (XRD) indicated that most of the clay was still stacked by co-coagulating agent while transmission electron microscopy (TEM) showed that some of the clay was exfoliated.

In this paper, SBR/clay nanocomposites were prepared by co-coagulating the mixture of rubber latex and clay aqueous suspension. Structure and properties of the nanocomposites were studied in detail, giving special attention to the clay- rubber interface. Structures of SBR/ clay nanocomposites were investigated for first time by tapping mode AFM.

Results and Discussion

Structure of SBR/clay nanocomposites

Qualitative understanding of the structure of nanocomposite through direct observation can be achieved by AFM image. On the other hand, XRD is a conventional method to determine the interlayer spacing of clay layers in the original clay and in the polymer/ layered silicate nanocomposite. The XRD patterns of the SBR/ Na-MMT nanocomposites and pure Na-MMT powder are presented in Fig. 1. Results in Fig. 1 suggest that in the nanocomposites prepared with less than 10 phr Na-MMT, silicate layers are completely exfoliated. Also, it is clear from Fig. 1 that the measured d_{001} basal spacing of sodium montmorillonite is 1.36 nm, whereas that in the nanocomposites with 10 and 20 phr Na-MMT is slightly larger (1.37 nm). It should be noted that with increasing the Na-MMT content from 10 phr to 20 phr, SBR/ Na-MMT nanocomposites show almost the same diffraction peak, indicating the same structure of nanocomposites obtained with 10 and 20 phr Na-MMT as it can be seen in AFM images (see Fig. 2) and mechanical property results (see the next section).

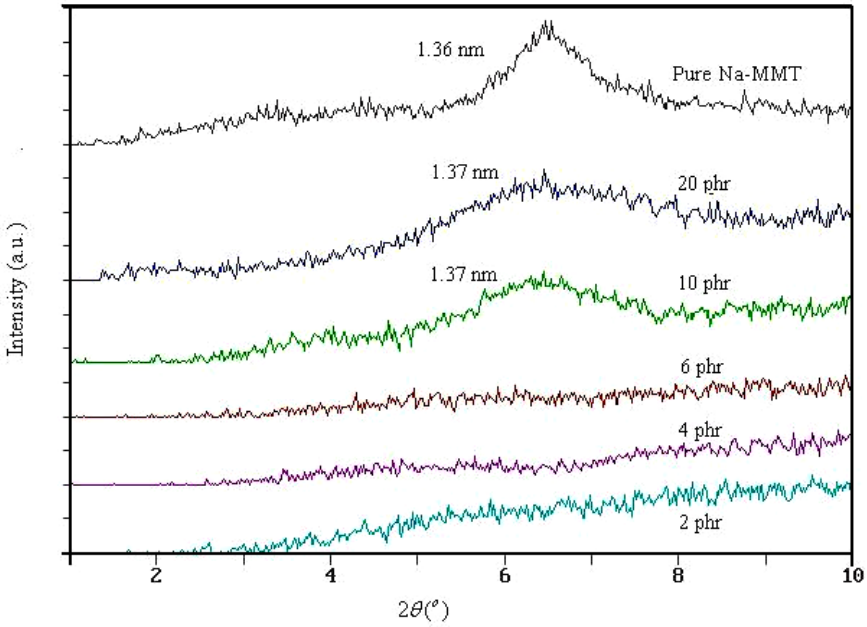

Fig. 1. XRD patterns for the pure Na-MMT and SBR/ Na-MMT nanocomposites.

Tapping mode AFM micrographs of SBR/ clay nanocomposites are shown in Fig. 2. The dark regions (hard layered silicates) are either the cross-sections (as the streaks) or the platelets (as the sheets) of (single or multiple) layered silicates and light regions are the soft rubber matrix [20, 22-23]. AFM height and phase images of the nanocomposite containing 2 phr clay are shown in Fig. 2a. It can be seen that the silicate layers (visible as dark sheets and streaks in the phase image) in the nanocomposites are dispersed in the rubber matrix with an average wide (length) from 0.1 to 1 μm. On the bases of XRD results, one can conclude that these dark sheets must be the single layers of silicates (with approximately 1 nm thick and 500 nm length). However, no significant exfoliated clay platelets with cross- sections of approximately 1-10 nm thickness are detected in the phase image. The only reason for this may be the lower resolution of AFM phase images, which makes it impossible to see the interface between single-layered silicate and rubber matrix. For this reason, the light regions in the phase image of nanocomposite containing 2 phr clay (Fig. 2a) seem to be single phase while on the bases of XRD pattern (Fig. 1), these regions may contain the single layers of silicates (with approximately 1 nm thickness) dispersed in the rubber matrix. Hence, phase images of the nanocomposites containing 10 and 20 phr Na-MMT (Figs. 2b and 2c respectively) reveal that a hybrid structure of mono-layered and multi-layered (streaks with thickness larger than 2 nm) silicates can be formed simultaneously in the nanocomposite with higher clay loading, consistent with exfoliated and non- exfoliated hybrid structure. Although there is no evidence but according to the XRD curves observed for nanocomposites containing 2, 4 and 6 phr Na-MMT, it was concluded that a partially exfoliated structure might be exist in the nanocomposites containing 10 and 20 phr. If intercalation of rubber chains into the interlayer of clay occurs, XRD peak will shift to a smaller angle for the intercalated nanocomposites, and if the Na-MMT layers are exfoliated completely, there will be no diffraction peaks observed because of the disorder of sheets or the larger space of the layers beyond the XRD resolution.

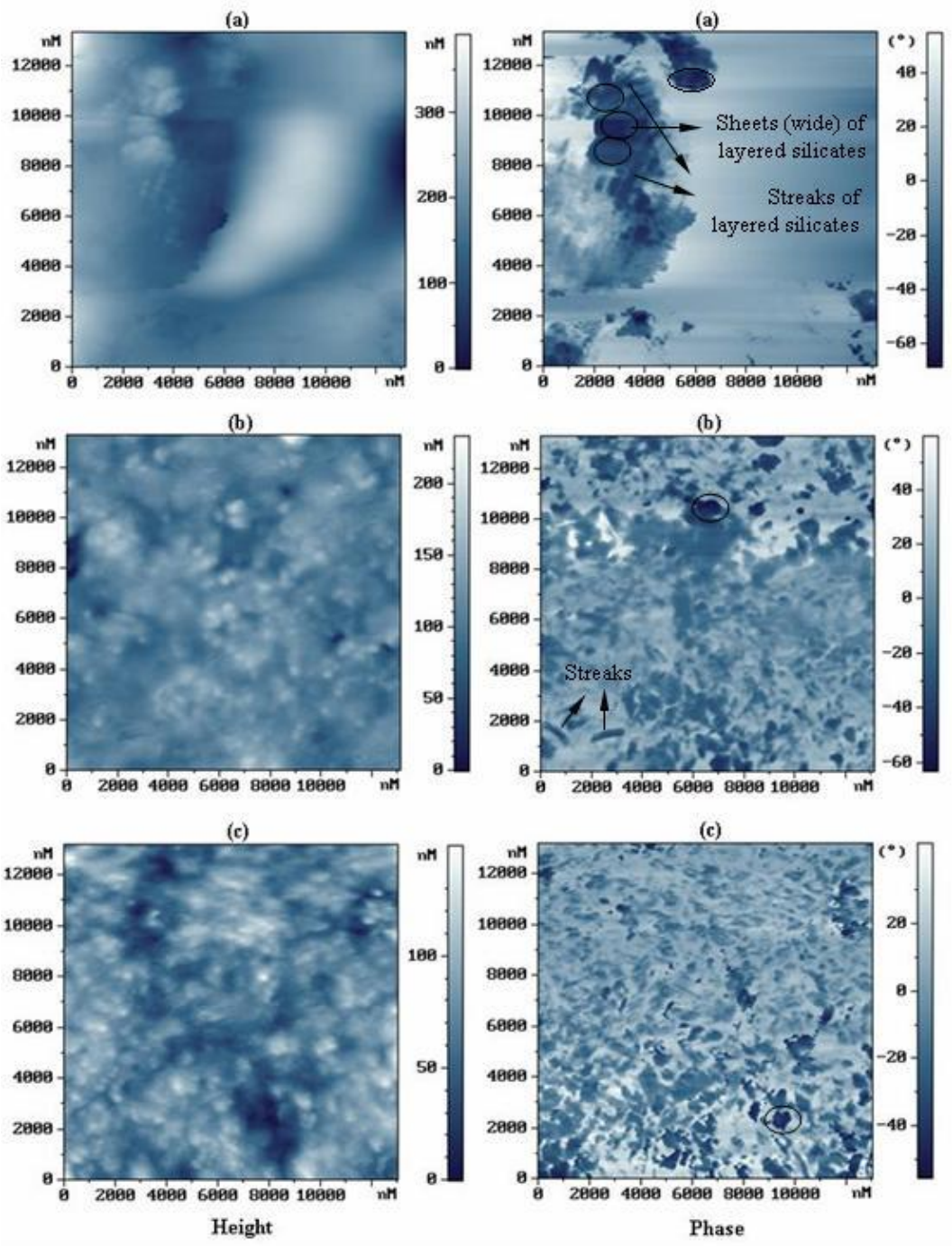

Fig. 2. AFM height (left) and phase (right) images of SBR/ Na-MMT nanocomposites containing (a): 2 phr Na-MMT, (b): 10 phr Na-MMT and (c): 20 phr Na-MMT prepared by co-coagulating the mixture of SBR latex and Na-MMT aqueous suspension.

However, in this study, the d_{001} basal spacing of the nanocomposites increased slightly, which would be too small for intercalation of rubber molecules into the space of Na-MMT. Slight increase of the d_{001} basal spacing may be explained by the introduction of the H^+ cations of flocculant different from the original ions (Na^+) existing in the gallery of the Na-MMT via a cation exchange reaction during the co-coagulation process. This nanodispersed structure without polymer chains

intercalated into intergallery is completely different from the well-known intercalated structure and exfoliated structure, which is apparently due to the unique preparation method. It has been investigated completely by Wang et al [24] as shown in Fig. 3. Based on the above results and Fig. 3, the dispersion phase of the nanocomposites prepared by latex compounding method involves the individual layer and nanoscale orderly stacking layers without polymer inserted. It is clear from Fig. 3 that the non-exfoliated layer aggregates in rubber/ clay nanocomposites prepared by co-coagulation the mixture of rubber latex and aqueous clay suspension are formed by the re-aggregation of clay layers during the co-coagulating process.

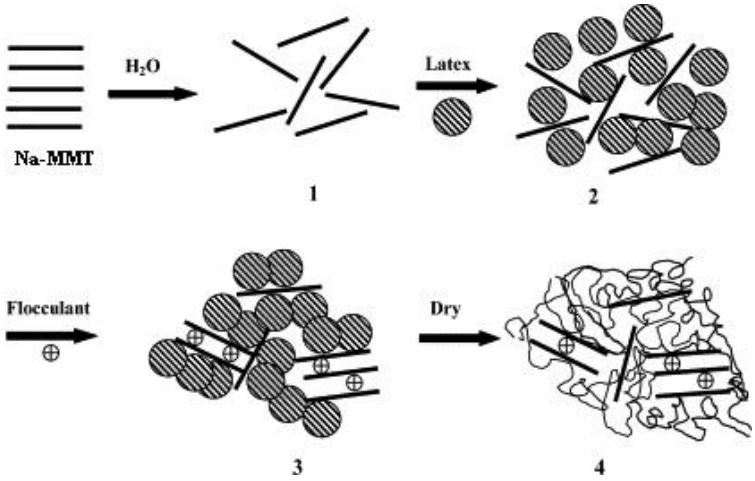

Fig. 3. Schematic illustration of the mixing and co-coagulating processes [24].

Dynamic Mechanical and Thermal Properties of SBR/ Clay nanocomposites

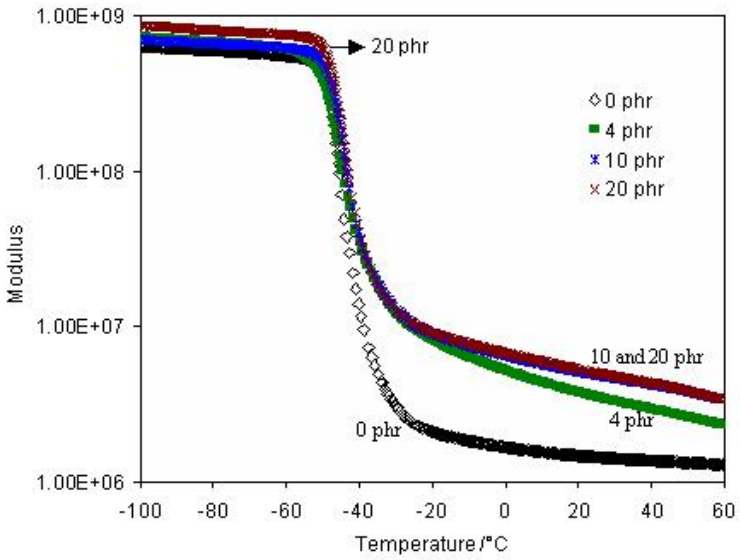

Fig. 4. The storage modulus versus temperature for clay- free SBR vulcanizate and SBR/ Na-MMT nanocomposites.

Dynamic mechanical properties are measured to investigate the degree of filler-matrix interaction of SBR/ Na-MMT nanocomposites. It should be noted that in order to investigate the general trend of Na-MMT content effect on dynamic mechanical properties, three nanocomposite samples along with the clay free SBR vulcanizate were selected as the representative samples among the five nanocomposite samples. The storage modulus of SBR filled with various amounts of clay versus temperature is shown in Fig. 4. The modulus of SBR/ clay nanocomposites is higher than that of clay free SBR vulcanizate, which further reflects the strong confinement of nano- dispersed silicate layers on the rubber chains. Moreover, the modulus of nanocomposites increases with increasing the clay content up to 10 phr and then become constant, which is consistent with the structure of nanocomposites observed by AFM and XRD. It indicates that the elastic responses of pure SBR towards deformation are influenced by the presence of nanodisperced Na-MMT layers especially completely exfoliated silicate layers. Improvement of storage modulus below T_g is slighter than above T_g, which is easy to be understood based on the mechanism of stress transfer of composites.

Fig. 5 shows the loss factor ($\tan\delta$) as a function of temperature. The SBR/ clay nanocomposites show the lower $\tan\delta$ value at the glass transition temperature than the clay free SBR vulcanizate. It can be attributed to the decreased mobility of rubber chains as restricted by silicate layers.

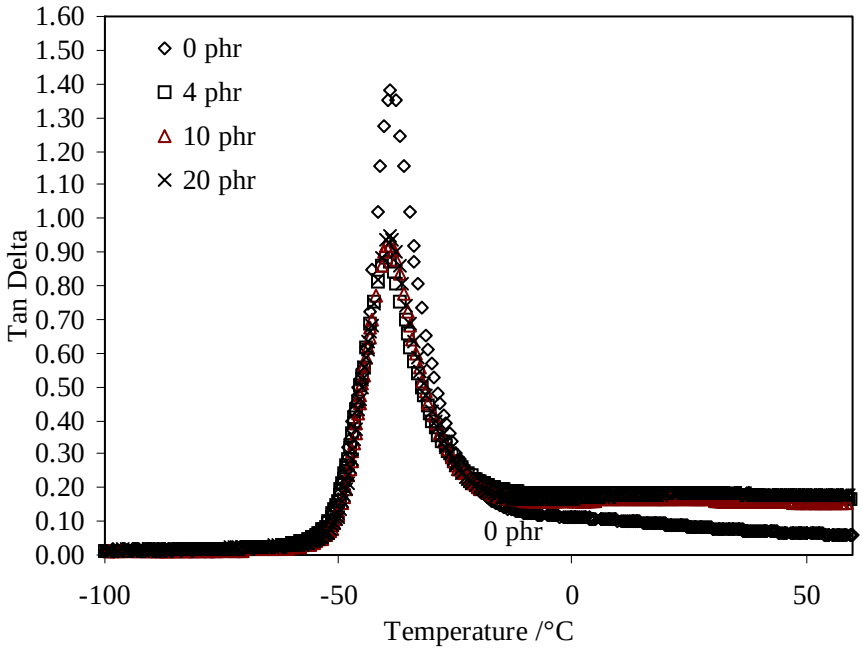

Fig. 5. $\tan\delta$ as a function of temperature for clay free SBR vulcanizate and SBR/ Na-MMT nanocomposites.

Amplitude of loss factor of SBR/ clay nanocomposites in the rubbery region (0-60 ^{o}C) become higher in comparison with the clay- free SBR vulcanizate, which suggests the stronger networking and the interfacial hysteresis originating from strong gradient confinement of rubber chains by silicate layers.

Thermal decomposition of nanocomposites was investigated by thermo-gravimetry analysis as shown in Fig. 6. Results show that the end decomposition temperature

shift to the higher values with increasing MMT loading; however, the presence of MMT does not affect the low temperature decomposition peak. The similar results have been observed for poly(ethyl acrylate)/ poly(methyl methacrylate) latex blends compounded with MMT [25]. This phenomenon is still being investigated. Moreover, although no significant changes were shown in the initial step of thermal degradation, the enhanced char yield was seen in the high temperature region with increasing clay content, which is in good agreement to the clay content. It should be noted that the char residue formation usually governs the flammability behavior of nanostructured materials.

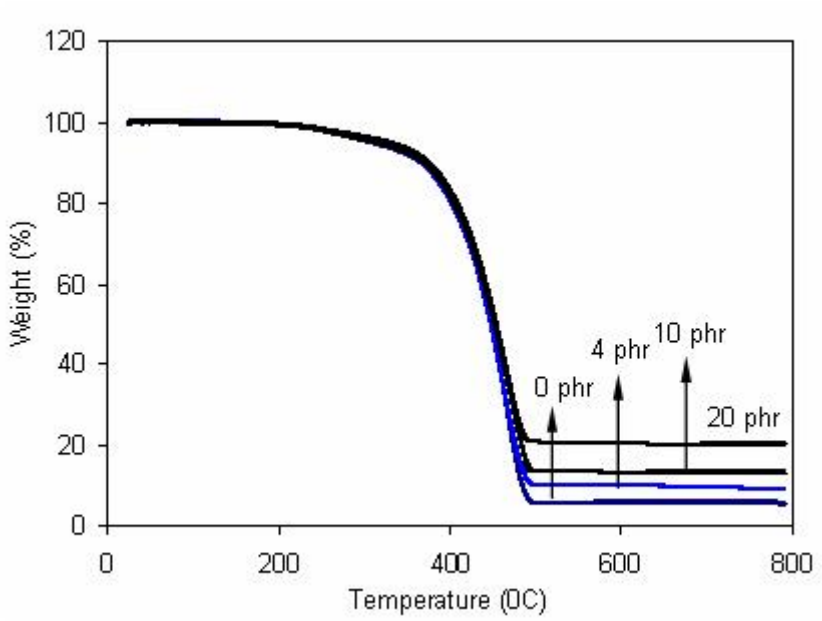

Fig. 6. TGA curves of pure NR and NR/Na-MMT nanocomposites.

Mechanical Properties of SBR/Clay nanocomposites

Fig. 7 shows the mechanical properties of SBR/Clay nanocomposites. The hardness (shore A) and 100 % tensile stress (i.e. tensile stress at 100% elongation) of nanocomposites (Fig. 7a) are higher than those of clay free SBR vulcanizate and also increased with increasing the amount of clay. It can be attributed to the layer structure of clay and extremely high interfacial action between the layer (or stacked layers) and rubber matrix. Fig. 7b shows that the tensile strength and tensile strain at break of SBR is improved by introducing the clay into the rubber matrix. In addition, the improvement increased by increasing the amount of clay in nanocomposites. The significant improvements of mechanical properties may give the evidence that both exfoliation and a large interface play critical roles in nano-reinforcement. The tear strength of nanocomposites (Fig. 7c) is very excellent in comparison with clay free SBR vulcanizate and increased with increasing the amount of clay. It was attributed to the special layer structure of the clay in the nanocomposites, the extreme interfacial interaction and the slide between the layer bundles, which could decrease the energy of the expansion of crack. It should be noted that all of the mechanical properties of nanocomposites improve considerably with increasing the clay content

up to 10 phr and then become less important, which is consistent with the structure of nanocomposites proposed by AFM and XRD results.

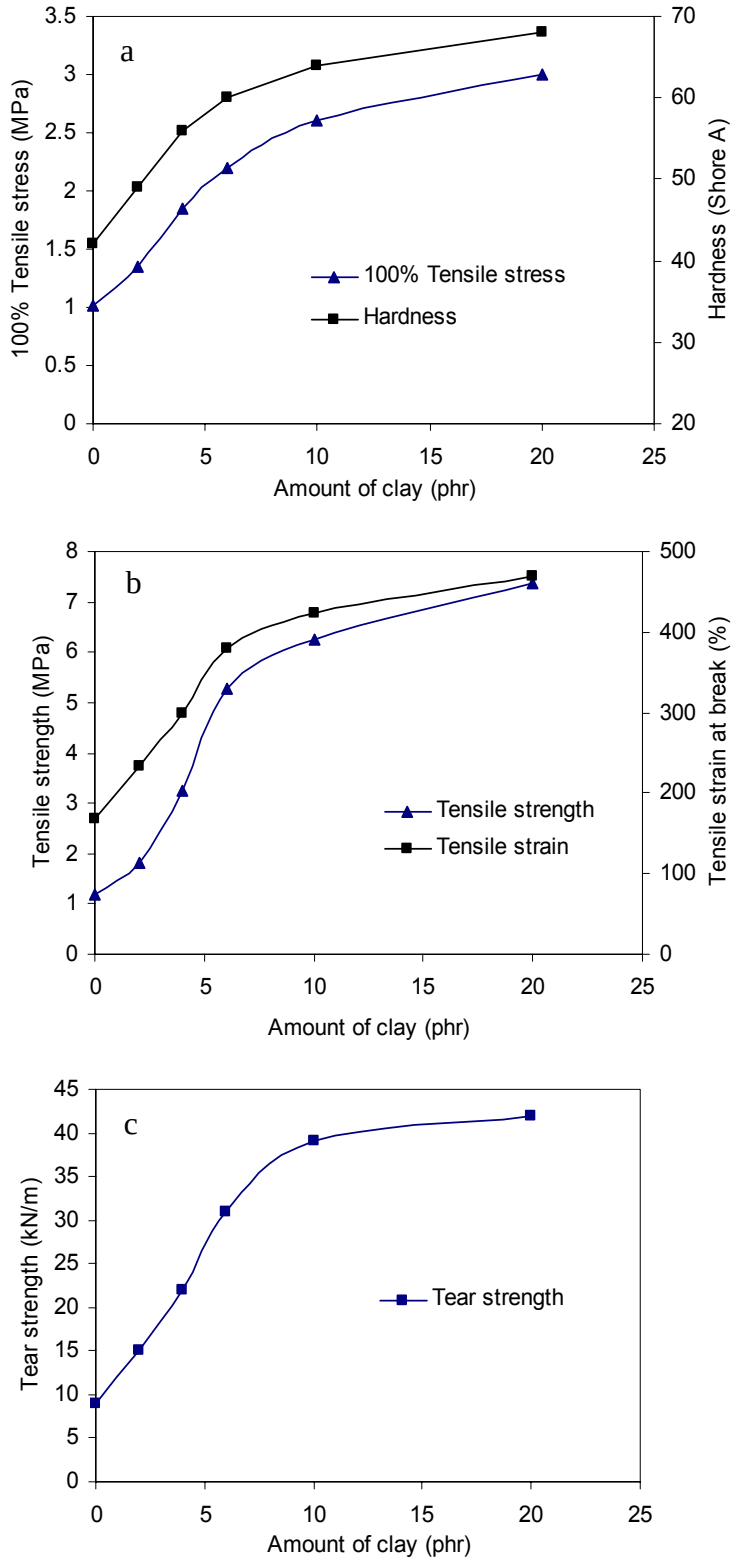

Fig. 7. Mechanical properties of clay free SBR vulcanizate and SBR/ Na-MMT nanocomposites.

Conclusions

SBR/ clay nanocomposites were prepared by co-coagulating the mixture of SBR latex and aqueous clay suspension. Tapping mode AFM and XRD were used to investigate the structure of nanocomposites. It was observed that the fully exfoliated structure could be obtained by this method only when the low content of layered silicates is used. SBR nanocomposites exhibit a lower $\tan\delta$ peak value, higher modulus and higher tan delta value at the rubbery region (0-60 ^{0}C) than the clay free SBR vulcanizate, which suggests the stronger networking and the interfacial hysteresis originating from strong gradient confinement of rubber molecules by silicate layers. Also, the nanocomposites have the higher hardness (shore A), 100% tensile stress, tensile strength, tensile strain at break and tear strength than the clay free SBR vulcanizate, which results from the nano-reinforcement effect of clay.

Experimental

Materials

Cloisite Na^+ (natural sodium-montmorillonite, Na-MMT) as a pristine clay with cation exchange capacity of 92 meq/100 gr of clay was provided by Southern clay products. SBR latex was available from Bandar Imam Petrochemical Co. (Iran) with the solid content of 17% and mean diameter of 79.0 nm. The rubber additives were of commercial grade, viz. zinc oxide, stearic acid, sulfur etc.

Preparation of SBR/ clay nanocomposites

Clay (Cloisite Na^+) was dispersed in deionized water with vigorous stirring by a special type of stirrer (Polytron, Switzerland) at a concentration of 2% and an aqueous suspension of layered silicate was obtained. Then, a given amount of SBR latex was added into the aqueous clay suspension and stirred for 30 min. Finally, the mixture was co-coagulated by cation-type coagulating agent (dilute solution of sulfuric acid, 2%), washed with water several times until its pH become 7 and then dried at 80 ^{0}C for 24 h. The SBR/clay nanocompounds were obtained.

To obtain the vulcanized nanocomposites, the above-mentioned nanocompounds as well as the clay free SBR were mixed with ingredients according to the recipe in Table 1 in a 6-inch two-roll mill; then the blends were vulcanized in a standard mold at 150 ^{0}C for the optimum cure time determined by a rheometer.

Tab. 1. Recipe for vulcanization of SBR/ Na-MMT nanocompounds.

Ingredients	Amounts (phr[a])
SBR	100
Cloisite Na^+	Variable
Zinc oxide	5.0
Stearic acid	2.0
Dibenzothiazole disulfide (DM)	0.5
Diphenyl guanidine (D)	0.5
Tetramethyl thiuram disulfide (TMTD)	0.2
Sulfur	2.0
N-isopropyl-*N'*-phenyl-*p*-phenylene diamine	1.0

[a] parts per hundred rubber

Characterization of the nanocomposites

An atomic force microscope (AFM, solver P47H supplied by NT-MDT Inc.) was used to map the distribution of clay platelets in the rubber matrix. Tapping mode AFM was used to obtain the phase images at the ambient temperature. It should be noted that the samples used in AFM and XRD analysis were the films obtained from casting the mixture of rubber latex and aqueous clay suspension while the samples used for other experiments were the sheets obtained from molding.

Thermogravimetric analysis (TGA) was performed under nitrogen purge on a Hi-Res TGA 2950 thermogravimetric analyzer (TA instruments) at a temperature range of 25-800 ^{o}C with heating rate of 20 ^{o}C/min.

X- ray diffraction (XRD) analysis was performed using a Philips Analytical X-ray diffractometer. An acceleration voltage of 40 kv and 25 mA were applied using Cu Kα radiation with wavelength λ = 0.154 nm. The diffraction curves were obtained within the range of scattering angles (2θ) of 2-10^{o} at a scan rate of 1^{o}/min.

Dynamic mechanical properties of vulcanized clay- free SBR and SBR/ clay nanocomposites were done using a dynamic mechanical thermal analyzer (DMTA, Rheometric Science Corp.) at a fixed frequency of 1 Hz with heating rate of 3 ^{o}C/min using liquid nitrogen for subambient temperature. Storage modulus and loss factors ($\tan\delta$) were obtained by rectangular tension mode.

Tensile and tear tests on the (at least five times) specimens were performed using a Zwick/Roell Tensile tester at a stretching speed of 500 mm/min for tensile test and 50 mm/min for tear test at the ambient temperature (25 ^{o}C) according to ISO 37-1994.

References

[1] Shelley, J.S.; Mather, P.T.; DeVries, K.L. *Polymer* **2001**, *42*: 5849.
[2] Joly, S.; Garnaud, G.; Ollirault, R.; Bokobza, L.; Mark, J.E. *Chem. Mater*. **2002**, *14*, 4204.
[3] Hamed, G.R. *Rubber Chem. Tech.* **2000**, *73*, 524.
[4] Karger- Kocsis, J.; Wu, C.M.; *Polym. Eng. Sci.* **2004**, *44*, 1083.
[5] Alexandre, M.; Dubois, P. *Mater. Sci. Eng., R: Reports*, **2000**, *28*, 1.
[6] Song, M.; Wong, C.W.; Jin, J.; Ansarifar, A.; Zhang, Z.Y.; Richardson, M. *Polym. Int.,* **2005**, *54*, 560.
[7] Kodgire, P.; Kalgaonkar, R.; Hambir, S.; Bulakh, N.; Jog, J.P. *J. Appl. Polym. Sci.* **2001**, *81*, 1786.
[8] Liu, L.; Jia, D.; Luo, Y.; Guo, B. *J. Appl. Polym. Sci.* **2006**, *100*, 1905.
[9] Ma, J.; Xu, J., Ren, J.H.; Yu, Z.Z.; Mai, Y.W. *Polymer* **2003**, *44*, 4619.
[10] Usuki, A.; Tukigase, S.; Kato, M. *Polymer* **2002**, *43*, 2185.
[11] Liu, L.; Luo, Y.; Jia, D.; Fu, W.; Guo, B. *J. Elast. Plast.* **2006**, *38*, 147.
[12] Abdollahi, M.; Khanbabae, G.; Rahmatpour, A.; Aalaie, J. *to be submitted*.
[13] Zhang, L.Q.; Wang, Y.Z.; Wang, Y.Q.; Sui, Y.; Yu, D. *J. Appl. Polym. Sci.* **2000**, *78*, 1873.
[14] Wang, Y.Z.; Zhang, L.Q.; Tang, C.; Yu, D. *J. ppl. Polym. Sci.* **2000**, *78*, 1879.
[15] Ma, J.; Xiang, P.; Mai, Y.W.; Zhang, L.Q. *Macromol. Rapid Commun*. **2004**, *25*, 1692.
[16] Wang, Y.Q.; Zhang, H.; Wu, Y.; Yang, J.; Zhang, L.Q. *J. Appl. Polym. Sci.* **2005**, *96*, 324.
[17] Jia, Q.X.; Wu, Y.P.; Xu, Y.L.; Mao, H.H.; Zhang, L.Q. *Macromol. Mater. Eng.* **2006**, *291*, 218.

[18] Wu, Y.P.; Zhang, L.Q.; Wang, Y.Q.; Liang, Y.; Yu, D.S. *J. Appl. Polym. Sci.* **2001**, *82*, 2842.
[19] Varghese, S.; Karger-Kocsis, J. *Polymer* **2003**, *44*, 4921.
[20] Dietsche, F.; Thomann, Y.; Thomann, R.; Mulhaupt, R. *J. Appl. Polym. Sci.,* **2000**, *75*: 396.
[21] Xu, Y.; Brittain, W.J.; Vaia, R.A.; Price, G. *Polymer* **2006**, *47*, 4564.
[22] Limary, R.; Swinnea, S.; Green, P.F. *Macromolecules* **2000**, *33*, 5227.
[23] Yalcin, B.; Cakmak, M. *Polymer* **2004**, *45*, 6623.
[24] Wang, Y.; Zhang, H.; Wu, Y.; Yang, J.; Zhang, L. *Eur. Polym. J.* **2005**, *41, 2776.*
[25] Xu, Y.; Brittain, W.J.; Vaia, R.A.; Price, G. *Polymer* **2006**; 47, 4564.